Induced contributions in the Rayleigh band of gaseous H_2S

Alessandra De Lorenzi, Alberto De Santis, Romana Frattini, and Marco Sampoli

Dipartimento di Chimica-Fisica, Università di Venezia, Dorsoduro 2137, 30123 Venezia, Italy

(Received 16 October 1985)

Polarized and depolarized rotational Raman spectra of gaseous H_2S have been measured at room temperature and different pressures, together with the Q branch of the ν_1 band used as an internal standard. Isotropic and anisotropic spectra are found to be affected by "collision"-induced effects which are not completely explainable in terms of the first-order dipole—induced-dipole (DID) mechanism. Integrated intensities, depolarization ratios, and spectral shapes are compared with theoretical predictions in order to discriminate between the different scattering mechanisms, which are accounted for in the framework of the multipolar and higher-order polarizability series expansion. Higher-order polarizabilities are considered for induced effects only, the laser power being fairly low. At the density considered, the anisotropic integrated intensity is due to ordinary rotational and induced contributions, the first-order DID one accounting for most of the measured intensity. Other induced contributions appear in the frequency range 100–450 cm^{-1}, the DID scattering being confined to low frequency. Their origin can be understood by analyzing the measured isotropic spectra. The rotational induced contribution involving the dipole-quadrupole polarizability tensor (αA contribution) is mainly responsible for the broad isotropic spectrum extending up to 450 cm^{-1}, whereas an induced contribution involving the first hyperpolarizability is negligible. It has been possible to estimate $A^2_{123,1} + A^2_{123,3} = 3$ Å^8. At the highest frequencies (300–450 cm^{-1}), the depolarization ratios and the comparison between experimental and theoretical αA spectra indicate the presence of other induced contributions which are likely due to the gradient of the quadrupolar field and to higher-order multipolar polarizabilities. The point-scatterer approximation of the multipolar series expansion is shown to reproduce the main spectral features. At low frequency, i.e., below 150 cm^{-1}, a sharp peak is found to be superimposed on the αA isotropic spectrum. The peak is likely due to higher-order DID effects, and to induced contributions involving second hyperpolarizability and long-range dispersion forces. Its origin is very similar to that of the isotropic spectrum of noble gases.

I. INTRODUCTION

In recent years many efforts have been devoted to the study of light scattering from fluids. To reproduce a given experimental spectrum, it would be necessary to know the scattering mechanisms and microscopic dynamics of the fluid which depend on the interaction potentials. Both the scattering mechanisms and interaction potentials are related to the electronic wave functions of the particles, so that some modeling is generally used for both.

In noble-gas fluids the central interaction potential is accurately determined as a function of interatomic distance. As regards the scattering processes, the first-order dipole—induced-dipole (DID) mechanism between point scatterers[1] has been found to explain surprisingly well the depolarized spectra[2,3] owing to some cancellation between higher-order DID and overlap contributions.[4,5] So it has been possible to reproduce the depolarized spectra satisfactorily[6,7] and to investigate the relations between spectral shapes and microscopic dynamics at the liquid density.[8,9] In fluids of linear molecules, quite reliable interaction potentials are available, and comparisons between real and simulated experiments have shown that induced effects are explained quite well by the DID mechanism between point polarizable particles in the case of small diatomics.[10]

For fluids consisting of globular molecules, namely octahedral and tetrahedral molecules, depolarized spectra show a rather sharp peak and very broad wings.[11-17] The central peak has been attributed to the usual DID mechanism between isotropic point scatterers, whereas the broad spectrum reflects the molecular nature of the fluid.[13] Stuckart et al.[18] have proposed that peripheral atoms rather than molecular centers interact via the first-order DID mechanism. This oversimplified model has been criticized by Buckingham and Tabiz since it does not reproduce the multipolar polarizabilities of the isolated molecule.[13] Recently, the possibility of applying a diffuse polarizability model to high-density fluids of globular molecules has been revised[19,20] on the basis of the atomic interacting site model of Silberstein[1] and Applequist et al.[21,22] In this form the model has also been applied to the scattering from dense fluids of elongated molecules with some success.[23-28] In the gas phase, the use of diffuse polarizability models is expected to be less crucial than in the liquid phase, owing to the greater mean intermolecular distance.[22] Indeed, if overlap and frame distortion contributions can be neglected, the molecular nature of the scatterers can be accounted for by polarizabilities of higher order and the long-range multipolar expansion around the molecular center. Recently, several comparisons between computed and measured low-density spectra

of globular molecules[13–17] have encouraged the interpretation of the spectra in terms of dipole-multipole polarizabilities. Besides, the study of the forbidden bands of CS_2, CO_2, and ethane fluids[29–32] has shown that the induced scattering can be explained through the dipole-multipole scattering mechanism, the contributions of the higher-order polarizabilities being negligible. Obviously, the long-range expansion approach is useful if the multipolar and higher polarizability series are quite rapidly convergent; otherwise, an effective polarizability model is compulsory in practice.

In this work we are dealing with rotational Raman spectra of gaseous H_2S, which for many aspects are less simple than the induced spectra of globular and linear molecules previously discussed. Indeed, the H_2S molecule has an exceptionally small optical anisotropy and a large isotropic polarizability,[33,34] so that both allowed and induced spectra are significant even at low density.[34–36] The low-frequency part of the anisotropic spectra is dominated by the DID contribution which completely obscures the allowed one.[35,34] At higher frequencies the rotational lines are clearly observable but an induced non-DID spectrum is present even at a few bars.[36] The study of such non-DID contributions can be more easily performed by analyzing the isotropic spectra which are entirely due to induced phenomena. Following this approach two of us have measured isotropic spectra of liquid H_2S and D_2S (Ref. 36) and suggested that induced rotational phenomena involving the dipole-quadrupole polarizability and the first hyperpolarizability could be responsible for the observed experimental findings.

The purpose of this work is to investigate the microscopic mechanisms giving rise to the polarized and depolarized light scattering from gaseous H_2S. This goal will be pursued by comparing experimental and theoretical integrated intensities, depolarization ratios, and line shapes.

II. BASIC THEORY

The contributions to light scattering due to multipole-multipole interactions and to polarizabilities of various order have been discussed extensively in the works of Buckingham,[37,38] Buckingham et al.,[13,39] and Kielich.[40] A formal theory has been subsequently developed by Samson et al.[41] Here we consider terms involving the polarizability α, the dipole-quadrupole polarizability $\mathbf{A}$, and the first two hyperpolarizabilities β and γ. For the estimate of induced effects the polarizability tensor of an H_2S molecule is assumed to be isotropic since induced contributions from the anisotropic part are expected to be very small in both isotropic and anisotropic spectra.[36] Cartesian components of the dipole μ and quadrupole Θ moments of the ith molecule are given by[38]

$$\mu_\alpha^{(i)} = \mu_\alpha^{0(i)} + \alpha^{(i)} E_\alpha + \tfrac{1}{3} A_{\alpha,\beta\gamma}^{(i)} E'_{\beta\gamma} + \tfrac{1}{2} \beta_{\alpha\beta\gamma}^{(i)} E_\beta E_\gamma$$
$$+ \tfrac{1}{6} \gamma_{\alpha\beta\gamma\delta}^{(i)} E_\beta E_\gamma E_\delta + \cdots , \tag{1}$$

$$\Theta_{\alpha\beta}^{(i)} = \Theta_{\alpha\beta}^{0(i)} + A_{\gamma,\alpha\beta}^{(i)} E_\gamma + \cdots , \tag{2}$$

where $\mathbf{E}$ and $\mathbf{E}'$ are the electric field and its gradient at the ith molecule, respectively. A pair of molecules i and j at the distance $\mathbf{R}_{ij} = \mathbf{R}_j - \mathbf{R}_i$ has an additional "induced" polarizability given by:[38,39,13]

$$^{TOT}\Pi_{\alpha\beta}^{(ij+ji)} = 2\alpha^{(i)}\alpha^{(j)} T_{\alpha\beta} + (\beta_{\alpha\beta\gamma}^{(i)} \mu_\delta^{0(j)} T_{\gamma\delta} + \beta_{\alpha\beta\gamma}^{(j)} \mu_\delta^{0(i)} T_{\gamma\delta}) + \tfrac{1}{2}(\gamma_{\alpha\beta\gamma\delta}^{(i)} E_\gamma^{(j)} E_\delta^{(j)} + \gamma_{\alpha\beta\gamma\delta}^{(j)} E_\gamma^{(i)} E_\delta^{(i)})$$
$$+ \tfrac{1}{3}[T_{\alpha\gamma\delta}(\alpha^{(i)} A_{\beta,\gamma\delta}^{(j)} - \alpha^{(j)} A_{\beta,\gamma\delta}^{(i)}) + T_{\beta\gamma\delta}(\alpha^{(i)} A_{\alpha,\gamma\delta}^{(j)} - \alpha^{(j)} A_{\alpha,\gamma\delta}^{(i)})] - \tfrac{2}{9} A_{\alpha,\eta\gamma}^{(i)} T_{\eta\gamma\delta\epsilon} A_{\beta,\delta\epsilon}^{(j)} + \cdots , \tag{3}$$

where $T_{\alpha_1\cdots\alpha_n}^{(n)}(R_{ij}) = [1/(4\pi\epsilon_0)]\nabla_{\alpha_1} \cdots \nabla_{\alpha_n}(1/R_{ij})$. The first term of Eq. (3) represents the well-known first-order DID contribution, the second and third terms refer to the nonlinear response of a molecule to the field originating from another molecule, the fourth one to the contributions from the induced quadrupolar field and gradient of the dipolar field, while the last one is due to the field gradient of the induced quadrupole. If Eq. (3) is transformed to spherical representation,[42] the expressions of the different contributions to the pair polarizability become

$$^{DID}\Pi_{12,M}^{(ij+ji)} = \frac{1}{4\pi\epsilon_0}[4\alpha^2 \mathscr{D}_{0,M}^{2*}(\Omega_{ij})R_{ij}^{-3}] , \tag{4}$$

$$^{\gamma E}\Pi_{10,0}^{(ij+ji)} = \gamma_{1010}^{(j)} \frac{1}{\sqrt{3}} \mathrm{Tr}(\mathbf{E}^{(i)}\mathbf{E}^{(i)}) , \tag{5}$$

$$^{\mu\beta}\Pi_{1K,M}^{(ij+ji)} = \frac{2\sqrt{10}}{4\pi\epsilon_0} \sum_l \sum_{\substack{m_1 m_2 \\ p_1,p_2 \\ s,q}} (-1)^{l-K+1} \left[\frac{2l+1}{2K+1}\right]^{1/2}$$
$$\times \langle l 1 m_1 m_2 | KM \rangle \langle 21 p_1 p_2 | 1 m_2 \rangle \mu_{1,s}^0 \beta_{1Kl,q} \mathscr{D}_{m_1,q}^{l*}(\Omega_i) \mathscr{D}_{p_2,s}^{1*}(\Omega_j) \mathscr{D}_{p_1,0}^{2*}(\Omega_{ij}) R_{ij}^{-3} , \tag{6}$$

$$^{\alpha A}\Pi_{1K,M}^{(ij+ji)} = \frac{2\sqrt{70}\alpha}{4\pi\epsilon_0} \sum_l \sum_{m_1 m_2 m} \sqrt{2l+1} W(213K;l1) \langle 3l m_2 m_1 | KM \rangle A_{12l,m}[\mathscr{D}_{m_1,m}^{l*}(\Omega_j) - \mathscr{D}_{m_1,m}^{l*}(\Omega_i)]\mathscr{D}_{m_2,0}^{3*}R_{ij}^{-4} , \tag{7}$$

$$^{AA}\Pi_{1K,M}^{(ij+ji)} = \frac{140\sqrt{2}}{4\pi\epsilon_0} \sum_{\substack{l_2l_3 \\ k_2k_3l}} (-1)^{-l_3}[(2l_2+1)(2l_3+1)(2k_2+1)(2k_3+1)(2l+1)]^{1/2}$$

$$\times W(11l_31;2l_2)W(21l_3K;l1)W(1142;k_23)$$

$$\times W(k_214l;k_32)\sum_{\substack{mn \\ \mu\rho\sigma}} \langle 4k_3\mu m \mid lq \rangle\langle l_3lnq \mid KM \rangle A_{1l_2l_3,\sigma}^{(i)}\mathscr{D}_{n,\sigma}^{3*}(\Omega_i)$$

$$\times A_{1k_2k_3,\rho}^{(j)}\mathscr{D}_{m,\rho}^{3*}(\Omega_j)\mathscr{D}_{\mu,0}^{4*}(\Omega_{ij})R_{ij}^{-5} , \qquad (8)$$

where $\mathscr{D}_{m,m'}^{n}(\Omega)$ stands for the rotation Wigner function and Ω_i and Ω_{ij} are sets of Eulerian angles specifying the orientations with respect to the laboratory frame of the ith molecule and the separation vector $\mathbf{R}_{ij}$.[43] The $\langle l_1l_2m_1m_2 \mid lm \rangle$ are Clebsch-Gordan coefficients and the $W(l_1l_2l_3l_4;l_5l_6)$ are Racah coefficients. For a generic tensor $\mathbf{B}$ of rank n, the different irreducible components of rank J_n are specified by the Stone notation $B_{1J_1}\cdots J_n$.[42] As regards $A_{1J_1J_2}$, which appears in Eqs. (7) and (8), it can be chosen as spherical component of either $A_{\alpha\beta,\gamma}$ or $A_{\gamma,\alpha\beta}$, owing to the symmetry properties of $\mathbf{T}^{(3)}$ and $\mathbf{T}^{(4)}$ tensors. The irreducible nth rank tensor $\mathbf{T}$ has been written in terms of the corresponding Wigner rotation function, namely,

$$T_m^{(n)}(\mathbf{R}) = \frac{C_n}{4\pi\epsilon_0}\mathscr{D}_{m,0}^{n*}(\Omega)R^{-(n+1)} , \qquad (9)$$

where C_n equals $\sqrt{6}$, $3\sqrt{10}$, and $6\sqrt{70}$ for $n=2,3,4$, respectively. For our purposes, only the rank zero (1010) component of γ has to be considered in Eq. (5). The nonzero Cartesian and spherical components of μ, β, γ, and A of the H_2S molecule and their literature values are reported in Appendix A.

At low densities, only two-body contributions are significant and for a system of N particles contained in a volume V, the correlation functions of the zz component of the total induced polarizability can be written as[44]

$$C_{VV}^{(K)}(t) = \frac{1}{V}\frac{N(N-1)}{2}\Phi_K\langle \Pi_{1K,0}^{(1,2+2,1)}(t)\Pi_{1K,0}^{(1,2+2,1)}(0)\rangle , \qquad (10)$$

where the values of Φ_K are $\frac{1}{3}$ and $\frac{2}{3}$ for $K=0$ and $K=2$, respectively.

For comparing theoretical and experimental results relative intensities will be calculated from

$$\tilde{I}_{VV}^{(K)} = \left| \frac{C_{VV}^{(K)}(0)}{\frac{N}{V}(\alpha_1')^2} \right| , \qquad (11)$$

where $(\alpha_1')^2 = (d\alpha/dq_1)^2\langle q_1^2 \rangle = 0.0225\mp0.0010$ cm^{-6} is the square of the isotropic polarizability derivative for the ν_1 symmetric stretching mode.[45]

III. EXPERIMENTAL AND RESULTS

A fairly conventional experimental apparatus has been used. An incident beam of a 171 Spectra Physics argon

ion laser having 3 W of power at 514.5 nm has been focused into a stainless-steel cell with fused quartz windows and Teflon gaskets. The 90° scattered light is analyzed by a Coderg T800 monochromator and detected by a low-noise cooled photomultiplier whose signal is processed by a single-photon counter and digitally recorded. Two samples of commercial H_2S gas (SIAD and Matheson), both of high purity (99.5%), have been used.

Spectra have been recorded at the pressure of 10, 11, and 16 bar at 296 K and at the pressure of 18 bar at 303 K. The temperature was kept within ∓1 K while the error of the pressure reading was about 2%. Density values have been deduced from PVT data of Ref. 46.

To obtain accurate depolarization ratios and isotropic spectra, errors due to the apparatus response are minimized by measuring polarized and depolarized spectra in VV and HV scattering geometry, respectively, i.e., by analyzing only the vertical component of the scattered light and by rotating the polarization of the incident laser beam from the vertical direction to that parallel to the scattering plane by means of the polarization rotator Spectra Physics (model 310-21).[47] Further, the collecting optics has a transfer ratio of about 1:1 and the very small solid angle $(1.1\times10^{-3}$ sr) of the reception cone leads to a leakage of the selected component into the unselected one lower than 3×10^{-3}. Usually, the investigated spectral range was 10–450 cm^{-1} of the Stokes side. The anti-Stokes side was evaluated following the detailed balance. In general, the resolving power was 7 cm^{-1} and the data have been recorded at fixed wavelengths every 2 cm^{-1}. The polarized Q branch of the ν_1 band has been measured before and after all spectral measurements.

Raw data are corrected for the overall apparatus response and for the trivial frequency factor of the Raman cross section. These corrections and the measurement of the intensity of the symmetric stretching Q band (whose linear density dependence[35] and Raman cross section[45] are known) allow to extract absolute or relative intensities.

In the present work only relative intensities defined by

$$\mathscr{I}_{band} = \frac{\mathscr{I}_{band}}{\mathscr{I}_{Q\ branch}^{\nu_1}} \qquad (12)$$

will be considered and compared with analogous theoretical expressions.

Figure 1 shows the depolarized HV spectra of gaseous H_2S together with the computed stick spectrum broadened

by a Gaussian line roughly reproducing the resolving power.[34,48] It can be seen that induced phenomena affect the allowed spectra everywhere. Although most of the intensity at low frequency may be attributed to the DID mechanism,[35] our spectra show a bump around 10 cm^{-1} (e.g., see Fig. 1, curve b) superimposed on the usual, nearly exponential noble-gas-like wing. A similar spectral shape has also been observed in neopentane vapor.[16] Further experimental data are shown in Fig. 2, where spectra obtained at two lower pressures (4 and 0.6 bar) are plotted. As is evident, the bump at 10 cm^{-1} becomes more and more pronounced as the density decreases, while the quasi stick spectrum shows no significant rotational transition below 30 cm^{-1}. Such a behavior could be ascribed to dimeric transitions as suggested by the theoretical spectra of argon.[49] Unfortunately, spectra at 0.6 bar of two commercial samples (SIAD and Matheson) with the same nominal purity differ significantly at low frequency, i.e., below 50 cm^{-1}, and we cannot state to what extent the impurity contributions have affected the spectral shapes of the dimer band envelopes.

From polarized VV and depolarized HV spectra, depolarization ratios and isotropic spectra have been derived (see Figs. 3 and 4) by means of the following equations:
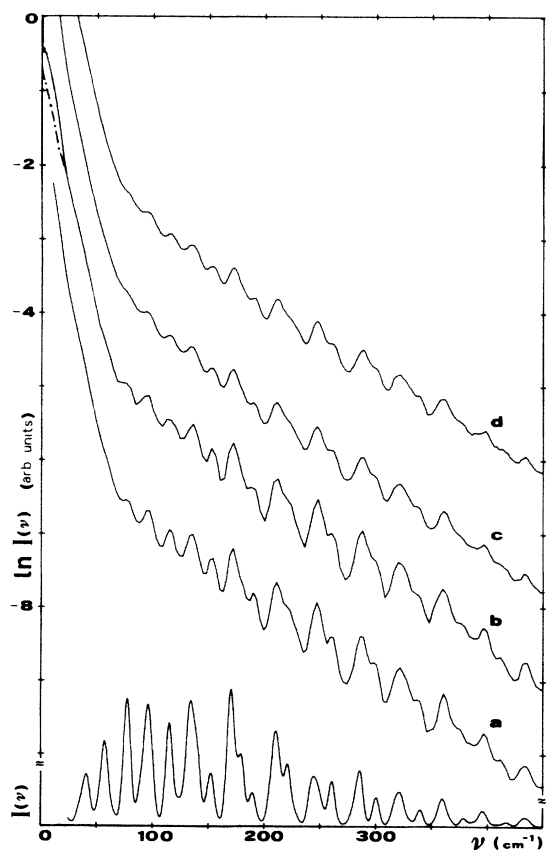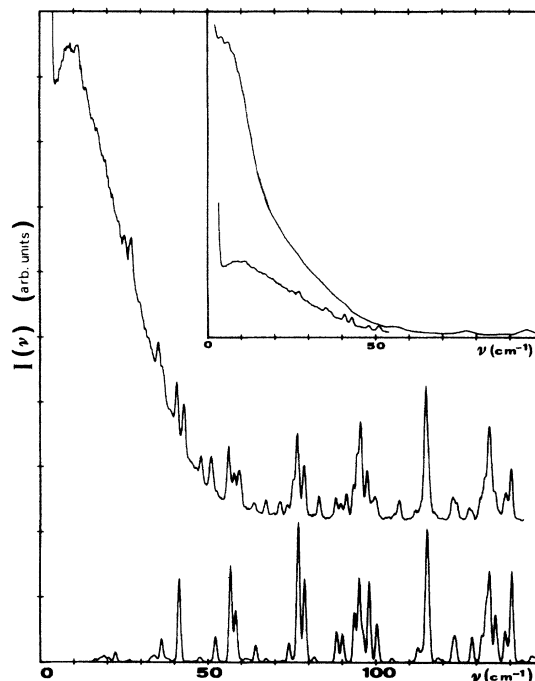

FIG. 2. Rayleigh spectrum of gaseous H₂S at room temperature and 0.6 bar (resolving power 1.5 cm^{-1}). The lowest spectrum is a broadened stick spectrum (Ref. 34). In the inset, the spectrum at 4 bar and room temperature (resolving power 0.8 cm^{-1}) is compared with the spectrum at 0.6 bar.

$$R(v) = \frac{\mathscr{I}_{HV}(v)}{\mathscr{I}_{VV}(v)}, \tag{13}$$

$$\mathscr{I}^{\text{iso}}(v) = \mathscr{I}_{VV}(v) - \tfrac{4}{3}\mathscr{I}_{HV}(v) \tag{14}$$

(note that some authors[6] use a different nomenclature, e.g., polarized for isotropic). The isotropic spectra show a peak below 100 cm^{-1}, and a broad spectrum. These two

FIG. 1. Depolarized Rayleigh spectra of gaseous H₂S (natural logarithmic scale) at room temperature and 10, 11, and 16 bar (a, b, and c, respectively), and at 303 K and 18 bar (d). The dashed-dotted part of curve b represents an extrapolation of the exponential trend. The lowest spectrum is a broadened stick spectrum (linear scale) computed as in Ref. 34.
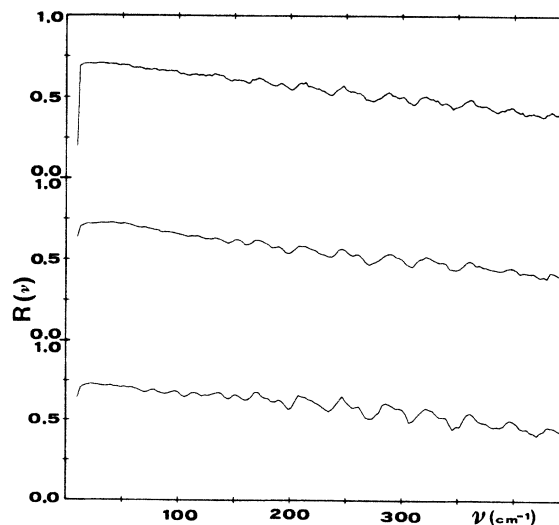

FIG. 3. Depolarization ratios vs frequency at 10 and 16 bar and room temperature and 18 bar and 303 K (from bottom to top). The result at 11 bar is not shown being practically equal to the result at 10 bar.
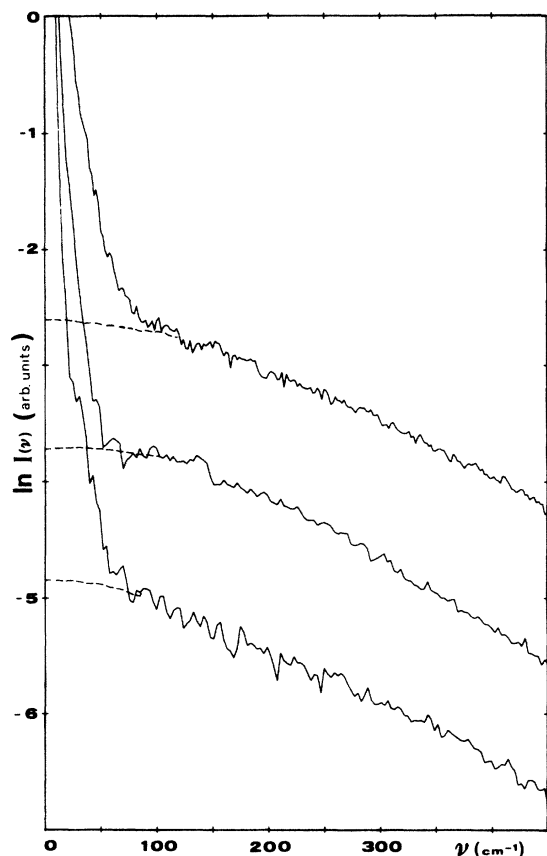
FIG. 4. Isotropic spectra of fluid H_2S at thermodynamic states as in Fig. 3, in the same order. The dashed lines represent a manual extrapolation separating the broad spectrum from the low-frequency peak.

features, also present in the spectra of the liquid,[36] have been separated by means of a flat extrapolation as shown in Fig. 4. The intensity of the broad spectrum ($\widetilde{\mathscr{J}}^{iso}_{broad}$) increases linearly with the density owing to the two-body character of induced effects at low densities. That is shown in Fig. 5, where we have also reported $\widetilde{\mathscr{J}}^{iso}_{broad}$ at 5 bar which has been evaluated from spectra that are relatively noisy but suitable for evaluating integrated intensities. The peak intensity ($\widetilde{\mathscr{J}}^{iso}_{peak}$) amounts to approximate-
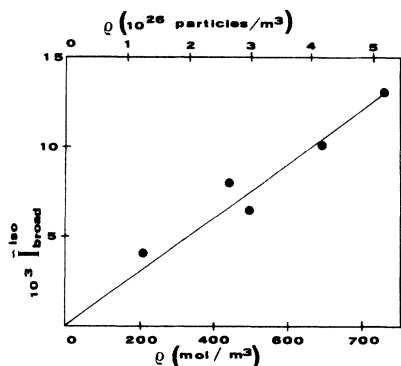

FIG. 5. Normalized intensity [Eq. (11)] of the broad isotropic spectra vs density. The solid line represents a manual "fit" of the data.

ly 1×10^{-2}, 3×10^{-2}, and 6×10^{-2} at 10, 16, and 18 bar, respectively, the error being at least 50%. That high uncertainty is due to both the zero-frequency interpolation for eliminating stray light and the Rayleigh-Brillouin signal, and to the smallness of the isotropic scattering with respect to the anisotropic one (see Fig. 3).

IV. SPECTRAL INTENSITIES AND DEPOLARIZATION RATIOS

Throughout this section orientational correlations between different molecules and correlations between orientations and translations are assumed to be negligible. Further, to evaluate the final formulas, the molecular properties of the H_2S molecule, reported in Table III (Appendix A) will be used.

A. The broad isotropic spectrum

The integrated intensity of the isotropic spectrum can be calculated from Eqs. (6), (7), (8), and (11). Equation (5), involving the second hyperpolarizability, gives contributions mainly at low frequency and will be discussed later. For the $\mu\beta$ and αA scattering mechanisms we have

$$\mu\beta\widetilde{\mathscr{J}}^{iso} = \frac{1}{(4\pi\epsilon_0)^2} \frac{4}{27} \frac{\rho(\mu^0)^2\beta^2}{(\alpha_1')^2} \langle R^{-6}_{1,2} \rangle , \tag{15}$$

$$\alpha A\widetilde{\mathscr{J}}^{iso} = \frac{1}{(4\pi\epsilon_0)^2} \frac{80}{63} \frac{\rho\alpha^2}{(\alpha_1')^2} (A^2_{123,1} + A^2_{123,3})\langle R^{-8}_{1,2} \rangle , \tag{16}$$

where ρ is the number density and $\beta = \sum_\alpha \beta_{y\alpha\alpha}$. The averages $\langle R^{-n}_{1,2} \rangle$ are given by

$$\langle R^{-n}_{1,2} \rangle = \frac{1}{(8\pi)^2} \int R^{-n}_{1,2} d\mathbf{R}_{1,2} \int g(\mathbf{R}_{1,2},\Omega_1,\Omega_2) d\Omega_1 d\Omega_2 . \tag{17}$$

No model for the anisotropic part of the intermolecular potential of H_2S is available. Therefore the isotropic 6–12 Lennard-Jones intermolecular potential with parameters $\epsilon/k_B = 300$ K and $\sigma = 3.49$ Å (Ref. 50) has been used. The classical low-density averages

$$\langle R^{-n}_{1,2} \rangle = 4\pi \int R^{-n}_{1,2}\exp[-U(R_{1,2})/k_BT]R^2_{1,2}dR_{1,2} \tag{18}$$

yield 0.19 Å^{-3}, 1.1×10^{-2} Å^{-5}, 6.9×10^{-4} Å^{-7}, and 4.6×10^{-5} Å^{-9} for $n = 6$, 8, 10, and 12, respectively.[51] The relative intensity of the $\mu\beta$ contribution is about 2 orders of magnitude smaller than the measurement (see Table I), and is practically negligible.

TABLE I. Relative intensities of the different induced isotropic contributions at $\rho = 3\times10^{26}$ particles/m^3 compared with the experimental data.

	$\mu\beta$	αA	AA [b]	$\widetilde{I}^{iso}_{peak}$
Theoretical[a]	3×10^{-5}	4×10^{-3}	9×10^{-7}	6×10^{-2}
Experimental	$\mathscr{J}^{iso}_{broad} = 7.5\times10^{-3}$		$\mathscr{J}^{iso}_{peak} = 1\times10^{-2}$	

[a]Relative intensities are calculated from Eq. (11).
[b]$l = 3$ components only.

The contribution of the αA mechanism cannot be appraised with the same accuracy, because the components of the **A** tensor of the H_2S molecule are unknown. We estimate the order of magnitude of **A** by using the site interaction model of Applequist *et al.*[21,22] The resulting values of the components $A^2_{123,\pm1}$ and $A^2_{123,\pm3}$ range from 0.56 to 0.80 and from -0.88 to -1.32 Å^4, respectively, for different choices of the site polarizabilities as discussed in Appendix A. Mean values $A_{123,\pm1}=0.67$ Å^4 and $A_{123,\pm3}=-1.07$ Å^4 yield an intensity quite consistent with the experimental findings (see Table I).

With regard to the intensity of the AA term [Eq. (8)] we note that all spherical components $l=1,2,3$ contribute, but their intensities are very small. Nevertheless, the contribution of the $l=3$ AA component term could be significant at very high frequency as discussed in Sec. IV C. We conclude that the αA mechanism accounts for the isotropic intensity of the broad spectrum; and 3 Å^8 is the value of $A^2_{123,1}+A^2_{123,3}$ matching with the experimental findings. The study of depolarization ratios and line shapes will support that conclusion.

B. Anisotropic spectral intensities

From Eqs. (4), (7), and (11) we get

$$^{\mathrm{DID}}\tilde{I}_{HV}=\frac{1}{(4\pi\epsilon_0)^2}\frac{6}{5}\frac{\rho\alpha^4}{(\alpha'_1)^2}\langle R^{-6}_{1,2}\rangle \ , \tag{19}$$

$$^{\alpha A}\tilde{I}_{HV}=\frac{1}{(4\pi\epsilon_0)^2}\frac{\rho\alpha^2}{(\alpha'_1)^2}[\tfrac{24}{35}A^2_{121,1}+\tfrac{16}{21}A^2_{122,1}$$

$$+\tfrac{16}{35}(A^2_{123,1}+A^2_{123,3})]\langle R^{-8}_{1,2}\rangle \ . \tag{20}$$

The anisotropic polarizability of the H_2S molecule can be written as

$$\alpha^{(i)}_{12,m}=\frac{2}{\sqrt{6}}\alpha_0\mathscr{D}^{2*}_{m,0}(\Omega_i)+\alpha_2[\mathscr{D}^{2*}_{m,2}(\Omega_i)+\mathscr{D}^{2*}_{m,-2}(\Omega_i)] \ , \tag{21}$$

where $\alpha_0=\frac{1}{2}(\alpha_{xx}+\alpha_{yy})-\alpha_{zz}$ and $\alpha_2=\frac{1}{2}(\alpha_{yy}-\alpha_{xx})$. The integrated depolarized rotational intensity is

$$^{\mathrm{rot}}I_{HV}\propto\frac{\rho}{15}(\alpha^2_0+3\alpha^2_2)=\frac{\rho}{15}\delta^2 \ . \tag{22}$$

The value of δ^2 is found to be dependent on the investigated frequency range or, more properly, on the distortion of the nuclear configuration.[52] A weighted average value of

0.6×10^{-51} cm^6 has recently been estimated.[34]

In Table II the reduced intensities $\tilde{I}_{HV}$ of the different contributions and experimental data are reported. The "experimental" DID intensity has been estimated from the low-frequency exponential trend of depolarized spectra. Experimental and theoretical results agree quite well and confirm that the DID mechanism is dominant and accounts for most of the total intensity even at few bars of pressure.[35] The contribution of αA is small with respect to the rotational one, so that the integrated experimental intensities are not very useful for an estimate of the extra-DID-induced components. A line-shape analysis, such as that performed in Refs. 17 and 54 for gaseous CH_4, appears to be difficult in the present case, since the presence of impurities and the quoted frequency dependence of δ^2 complicate the separation of extra-DID contributions from DID and rotational ones.

C. Depolarization ratio

Further information about the nature of the induced effects can be obtained from the frequency dependence of the depolarization ratio $R(\nu)$ shown in Fig. 3. The oscillations over the decreasing profile correspond to the frequencies of the rotational transitions[34] which, being completely depolarized, provide a local increase of the depolarization ratio. To understand the decreasing trend of $R(\nu)$ both the VV and HV polarizability correlation functions of the induced effects have been analyzed. Only the component $A_{123,m}$ contributes to the isotropic spectrum, while the other contributions, due to $A_{121,m}$ and $A_{122,m}$ are completely depolarized. The spectra involving these tensors cover a smaller frequency range; consequently, we expect that $R(\nu)$ decreases monotonically to a limit represented by the high-frequency depolarization ratio of the αA_{123} spectrum. This limit can be estimated with the hypothesis of uncorrelated orientations previously mentioned. From Eqs. (7) and (10) one obtains

$$^{\alpha A_{123}}C^{(K)}_{VV}(t)=\frac{\rho^2}{(4\pi\epsilon_0)^2}g_K\alpha^2\left\langle\frac{\mathscr{D}^3_{0,0}[\delta\Omega_{1,2}(t)]}{R^4_{1,2}(t)R^4_{1,2}(0)}\right\rangle$$

$$\times\sum_m(A_{123,m})^2\langle\mathscr{D}^3_{m,m}[\delta\Omega_1(t)]\rangle \ , \tag{23}$$

where $\delta\Omega$ specifies the zero time relative orientation and g_K takes the values $\frac{40}{63}$ and $\frac{32}{105}$ for $K=0$ and 2, respectively, in agreement with the results of Refs. 13 and 15. Equation (23) leads to a depolarization ratio

$$R_{\alpha A}(\nu)=3I^{(2)}_{VV}(\nu)/4[I^{(2)}_{VV}(\nu)+I^{(0)}_{VV})(\nu)]=\frac{9}{37}$$

TABLE II. Depolarized experimental and theoretical relative intensities [Eqs. (12) and (11)] at $\rho=3\times10^{26}$ particles/m^3.

	DID	αA_{121}	αA_{122}	αA_{123}	Rotational	Total
Experimental	0.53[a]					0.56[a]
Theoretical	0.58[b]	1×10^{-3}	1×10^{-5}	2×10^{-3}	2×10^{-2}	0.60

[a]The quoted error is about 10%, mainly due to zero-frequency extrapolation.
[b]The two values of α reported in Ref. 53 yield an uncertainty of 12%.

independent of frequency.

The experimental value is about 0.4 at 450 cm^{-1} and has been found to be nearly constant around 0.35 in the range 600–650 cm^{-1}.[36] Such a value is a bit larger than the theoretical prediction. This fact could be explained by considering the role of the AA contribution due to the $A_{123,m}$ spherical component. The spectra of such a term extend at very high frequencies since they involve double rotational transitions.[13,17] From Eqs. (8) and (10) one has

$$^{AA}C_{VV}^{(K)}(t) = \frac{\rho^2}{(4\pi\epsilon_0)^2} f_K \left\langle \frac{\mathscr{D}_{0,0}^4[\delta\Omega_{1,2}(t)]}{R_{1,2}^5(t)R_{1,2}^5(0)} \right\rangle$$

$$\times \sum_m (A_{123,m}^{(1)})^2 \langle \mathscr{D}_{m,m}^3[\delta\Omega_1(t)] \rangle$$

$$\times \sum_n (A_{123,n}^{(2)})^2 \langle \mathscr{D}_{n,n}^3[\delta\Omega_2(t)] \rangle , \qquad (24)$$

where f_K takes the values $\frac{176}{5103}$ and $\frac{31456}{127575}$ for $K=0$ and 2, respectively, in agreement with the calculations of Ref. 13. That leads to a constant $R_{AA}(\nu)=0.658$. Therefore, the AA contribution rises $R(\nu)$ at high frequency in qualitative agreement with the experimental findings.

D. The isotropic low-frequency scattering

A strong increase of intensity with decreasing frequencies is observed at low frequency in all spectra of Fig. 4.

Such a feature has been found in spectra of liquid H$_2$S, too.[36] It can be related neither to the αA mechanism whose spectrum is nearly flat at low frequency (see Sec. V), nor to the $\mu\beta$ mechanism whose intensity is too small to be responsible for $\mathscr{I}_{\text{peak}}^{\text{iso}}$ (see Table I). Between the DID terms only the ones beyond first-order contribute to the isotropic spectrum as in the case of noble gases (see Appendix A). Indeed, the very small permanent polarizability anisotropy makes the first-order DID contribution completely negligible.

To reproduce the isotropic spectra of the noble gases the isotropic pair polarizability is usually modeled by[6,37]

$$a^{(ij+ji)} = A^{(ij)} - T_0 \exp\left[-\frac{R_{ij}}{R_t} \right] ,$$

$$A^{(ij)} = \frac{4\alpha^3}{4\pi\epsilon_0 R_{ij}^6} + \frac{5}{9}\gamma E_{\text{disp}}^2 , \qquad (25)$$

where the exponential represents the electronic overlap contribution and $A^{(ij)}$ takes into account the DID long-range expansion of Eq. (A8) and dispersion forces contribution. In principle, in the case of H$_2$S, electrical fields due to the molecular permanent multipoles have to be considered, too. Owing to the strong H$_2$S dipole moment, only the dipolar electrical field is considered in the pair polarizability:

$$a^{(ij+ji)} = \frac{4\alpha^3}{4\pi\epsilon_0 R_{ij}^6} + \frac{5}{9}\gamma E_{\text{disp}}^2 + \frac{1}{4\pi\epsilon_0 R_{ij}^6}\{ \tfrac{5}{9}(\mu^0)^2\gamma[\mathscr{D}_{0,0}^2(\Omega_i)+\mathscr{D}_{0,0}^2(\Omega_j)+2]\} - \mathscr{F} , \qquad (26)$$

where $\mathscr{F}$ is a function accounting for electronic overlap contributions at short range. The first term is "fluctuating" with the intermolecular distance, whereas the dipolar term involves molecular orientational "fluctuations" too. However, the intensity contributions of the second one are relatively small at both the low- and high-frequency ends of the isotropic spectrum, and will be neglected together with the contributions from $\mathscr{F}$ since an estimate of $\mathscr{F}$ is not available at the present. If E_{disp}^2 is estimated classically[37] by using the 6–12 Lennard-Jones isotropic intermolecular potential of Table III, the following reduced intensity results:

$$\widetilde{I}_{\text{peak}}^{\text{iso}} \cong \frac{1}{(4\pi\epsilon_0)^2} \frac{\rho}{2(\alpha_1')^2} \langle R_{1,2}^{-12} \rangle \left[4\alpha^3 + \frac{20}{9}\gamma\frac{\epsilon\sigma^6}{\alpha} \right]^2 . \qquad (27)$$

The value of $\widetilde{I}_{\text{peak}}^{\text{iso}}$ reported in Table I is of the same order of magnitude as the experimental $\mathscr{I}_{\text{peak}}^{\text{iso}}$. It is reasonable to conclude that the $\mathscr{I}_{\text{peak}}^{\text{iso}}$ can be ascribed to the same translational phenomena which generate isotropic light scattering in monatomic fluids. That is also confirmed by the similarity of the low-frequency isotropic spectra of liquid H$_2$S and D$_2$S.[36]

V. SPECTRAL LINE SHAPE

The theoretical isotropic spectrum of the αA contribution at low density is given by

$$^{\alpha A}I^{\text{iso}}(\nu) \propto \frac{40\rho^2\alpha^2}{63(4\pi\epsilon_0)^2} \langle R_{1,2}^{-8} \rangle \sum_{rr'} g_r \exp\left[-\frac{E_r}{k_B T} \right] \left| \sum_p A_{123,p} W_{r',r}^p \right|^2 \delta\left[\nu - \frac{(E_{r'}-E_r)}{hc} \right] \otimes G_3(\nu) . \qquad (28)$$

The derivation of Eq. (28) is discussed in Appendix B. In general, $G_n(\nu)$ is a unit area function related to translational dynamics and proportional to the Fourier transform of the correlation function of $\mathscr{D}_{0,0}^n(\Omega_{1,2})/R_{1,2}^{n+1}$. Low-density line shapes in the cases

$n=2,3,4$ have been recently reported for an effective spherical intermolecular potential.[16] It appears that the $n=3$ and 2 spectra differ significantly, the $n=2$ spectra being about 50% larger and less enhanced at low frequency. We have found that the empirical line shape

TABLE III. Molecular properties of the H_2S molecule.

Molecular parameters			
Bond length[a]	Bond angle[a]	LJ (6-12) parameters[b]	
1.3518 Å	92.13°	$\epsilon/k = 300$ K, $\sigma = 3.49$ Å	

Molecular properties	Symmetry properties	Nonzero Cartesian components[c]	Nonzero spherical components[h]
Dipole moment μ 1 Cm $= 2.998 \times 10^{11}$ esu		$\mu_y = 0.974 \times 10^{-18}$ esu[d]	$\mu_{1,\pm1} = \dfrac{1}{\sqrt{2}} \mu_y$
Polarizability α 1 $C^2 m^2 J^{-1} = 8.988 \times 10^{15}$ cm^3	$\alpha_{\alpha\beta} = \alpha_{\beta\alpha}$	$\alpha_{xx} = 3.753 \times 10^{-24}$ cm^{3e} $\alpha_{yy} = 3.736 \times 10^{-24}$ cm^3 $\alpha_{zz} = 3.821 \times 10^{-24}$ cm^3	$\alpha_{10,0} = \dfrac{1}{\sqrt{3}} \sum_\alpha \alpha_{\alpha\alpha} = \sqrt{3}\alpha$ $\alpha_{12,\pm2} = -\frac{1}{2}(\alpha_{xx} - \alpha_{yy}) = \alpha_2$ $\alpha_{12,0} = -(\frac{2}{3})^{1/2}[\alpha_{zz} - \frac{1}{2}(\alpha_{xx} + \alpha_{yy})]$ $\quad = \sqrt{2/3}\alpha_0$
Quadrupole polarizability A 1 $C^2 m^3 J^{-1} = 8.988 \times 10^{17}$ cm^4	$A_{\alpha\beta,\gamma} \equiv A_{\gamma,\alpha\beta}$ $A_{\alpha\beta,\gamma} = A_{\beta\alpha,\gamma}$ $A_{\alpha\alpha,\gamma} = 0$	$A_{xx,y}, A_{yy,y}, A_{xy,x}, A_{zy,z}$	$A_{121,\pm1} = \dfrac{1}{\sqrt{30}}(2A_{yy,y} - A_{xx,y} - A_{zz,y})$ $\qquad\qquad + 3(A_{xy,x} + A_{zy,z})$ $A_{122,\pm1} = \mp\dfrac{1}{\sqrt{6}}(A_{zy,z} + A_{xx,y} - A_{zz,y} - A_{xy,x})$ $A_{123,\pm1} = \dfrac{1}{\sqrt{120}}(3A_{yy,y} + A_{xx,y} - 4A_{zz,y}$ $\qquad\qquad + 2A_{xy,x} - 8A_{zy,z})$ $A_{123,\pm3} = \dfrac{1}{\sqrt{8}}(A_{yy,y} - A_{xx,y} - 2A_{xy,x})$
First hyperpolarizability β 1 $C^3 m^3 J^{-2} = 2.694 \times 10^{20}$ esu	Symmetry in all suffixes	$\beta_{yxx}, \beta_{yyy}, \beta_{yzz}$ $\beta = \sum_\alpha \beta_{y\alpha\alpha} = -2.7 \times 10^{-31}$ esu^f	$\beta_{101,\pm1} = \dfrac{1}{\sqrt{6}}\beta$ $\beta_{121,\pm1} = (\frac{2}{15})^{1/2}\beta$ $\beta_{123,\pm1} = \dfrac{3}{\sqrt{120}}(\beta - 5\beta_{yzz})$ $\beta_{123,\pm3} = \dfrac{1}{\sqrt{8}}(\beta_{yyy} - 3\beta_{yxx})$
Second hyperpolarizability γ 1 $C^4 m^4 J^{-3} = 8.078 \times 10^{24}$ esu	Symmetry in all suffixes	$\gamma_{xxxx}, \gamma_{yyyy}, \gamma_{zzzz}$ $\gamma_{xxyy}, \gamma_{zzyy}, \gamma_{xxzz}$ $\gamma = \frac{1}{5}\sum_{\alpha\beta}\gamma_{\alpha\alpha\beta\beta}$ $\quad = 5.19 \times 10^{-36}$ esu^g	$\gamma_{1010} = \frac{5}{3}\gamma, \ldots$

[a]Reference 67.
[b]Reference 50.
[c]Tensor components refer to the III^r representation (Y axis along the dipole moment, Z axis out of plane, right-handed frame).
[d]Reference 68.
[e]Reference 34.
[f]Reference 69.
[g]Reference 70.
[h]Following the Stone notation (Ref. 42) and the Fano Racah's phase convention.

$$G_3(v) = B\left[1 - 0.5\exp\left(-\dfrac{|v|}{\Delta}\right)\right]\exp\left(-\dfrac{|v|}{\Delta}\right) \qquad (29)$$

used elsewhere to simulate collision-induced profiles of linear molecules[55] reproduces quite well the shape of $G_3(v)$ of Ref. 16. That line shape has been used to convo-

lute the αA stick spectrum of H_2S. The translational broadening parameter Δ has been set to 25 cm^{-1} in agreement with the width of $G_2(v)$ estimated from the anisotropic DID spectrum (exponential slope of 15 cm^{-1} at 11 bar). Figure 6 shows some broadened αA spectra corresponding to different choices of $A_{123,1}$ and $A_{123,3}$ togeth-
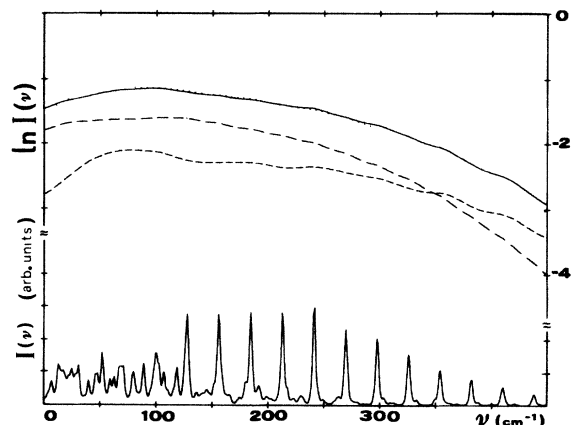
FIG. 6. Quasi stick αA spectrum (linear scale) of the H_2S molecule, calculated with $A_{123,3}/A_{123,1} = -1.5$. The upper curves represent the broadened stick spectrum (logarithmic scale) calculated for the following different values of $A_{123,1}$ and $A_{123,3}$: (————) and (· · · ·) refer to $A_{123,3}/A_{123,1}$ equal to 1 and -1, respectively; (— — —) is due to $A_{123,1}$ only and (—·—·—·) to $A_{123,3}$ only.

FIG. 7. The experimental broad spectrum (————) at 18 bar and 303 K, compared with theoretical αA spectrum (· · · ·) calculated with $A_{123,3}/A_{123,1} = -1.5$. Manual extrapolation (— — —) as in Fig. 4.

er with a quasi stick spectrum. It is worth noting that the strong peak structure of the quasi stick spectrum is completely obscured by the translational broadening. Figure 7 compares the experimental H_2S spectrum at 18 bar with the theoretical one calculated with $A_{123,3}/A_{123,1} = -1.5$, a ratio close to model predictions (see Table IV). The theoretical line shape reproduces the experiment in the range 150–300 cm^{-1}. Obviously, the disagreement at low frequency can be attributed to the rough separation of the experimental data into a broad spectrum and a low-frequency peak. Beyond 300 cm^{-1} there is a considerable excess of experimental intensity, and part of it might be ascribed to a smaller value of $|A_{123,3}/A_{123,1}|$ (see Fig. 6).

In the depolarized spectra of globular molecules,[13–17] the scattering from double AA transitions and dipole octopole polarizability is necessary to explain the intensity excess at high frequency. In our case the presence of high-frequency contributions has been brought to light by
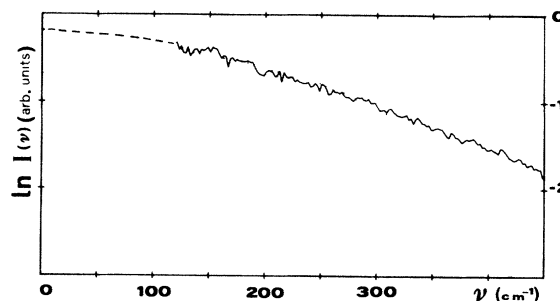
the analysis of the depolarization ratios. However, before considering other scattering mechanisms, it would be necessary to know a more reliable interaction potential and understand the limit of the hypothesis of uncorrelated molecular orientations in the case of a strongly dipolar fluid such as H_2S.

VI. SUMMARY AND CONCLUSIONS

In the present work different scattering mechanisms have been analyzed in order to interpret the measured isotropic and anisotropic spectra of gaseous H_2S. The anisotropic integrated intensity is almost entirely due to the first-order DID mechanism, the allowed and other induced contributions being small. Nevertheless, the extra DID terms have non-negligible effects on the high-frequency spectral wings, the DID scattering and most of the rotational spectrum being confined to frequencies below 200 cm^{-1}.

The comparison between experimental and theoretical intensities of the isotropic scattering, which is due to induced phenomena beyond first-order DID, has permitted the identification of the main scattering mechanisms. For many aspects, the isotropic spectrum is found to be similar to the depolarized spectra of globular molecules (CH_4 in particular). Indeed, the contribution due to the first

TABLE IV. Atomic site polarizabilities and values of the components of tensor A for H_2O and H_2S molecules.

α_1[a]	α_2	$A_{y,yy}$	$A_{y,xx}$	$A_{x,xy}$	$A_{z,zy}$	$A_{121,1}$	$A_{122,1}$	$A_{123,1}$	$A_{123,3}$
				H_2O					
		0.172[b]	0.147	0.52	0.14	0.46	0.04	0.17	−0.36
0.135[c]	0.465[c]	0.11	0.27	1.17	0.13	0.77	0.16	0.32	−0.89
				H_2S					
0.135	2.7	0.27	0.70	1.66	−0.01	1.06	-2×10^{-8}	0.80	−1.32
0.11	2.85	0.22	0.58	1.34	−0.03	0.84	-4×10^{-5}	0.67	−1.07
0.065	3.2	0.18	0.48	1.09	−0.04	0.67	0.14	0.56	−0.88

[a] α_1 is the site polarizability of hydrogen.
[b] All data of this row are the results of *ab initio* calculations of Ref. 59. The A components are in Å^4 units.
[c] Site polarizabilities from Ref. 21, in Å^3 units.

hyperpolarizability and the dipole moment is found to be negligible, whereas the ones due to the isotropic and dipole-quadrupole polarizabilities can explain the observed broad spectrum. It has been possible to estimate $A_{123,1}^2 + A_{323,3}^2 = 3$ Å^8, but the presence of other induced contributions in the far wings prevents evaluation of each component separately.

The low-frequency part $(\nu < 100$ cm$^{-1})$ of the isotropic spectrum is dominated by excess scattering intensities explainable in terms of pure translational contributions (a noble-gas-like spectrum), namely, second-order DID and dispersion forces. To our knowledge, this is the first experimental study of such an isotropic translational spectrum in molecular fluids, while the isotropic spectra of noble gases have been investigated extensively by Fromm-hold, Proffitt, and co-workers.[3,6] Its relatively easy measurement is due to some favorable circumstances found in H₂S. With respect to noble gases the H₂S molecule has larger α and γ values, and its molecular anisotropy of the polarizability is so small that the first-order DID contribution is absolutely negligible. In principle, we expect that strong isotropic translational spectra might be observed in globular and linear molecules. But in these cases highly polarizable molecules (e.g., CCl₄, neopentane, and CS₂) have high moments of inertia so that the induced rotational and translational spectra occur in nearly the same frequency range and may be difficult to separate.

In conclusion, the leading mechanisms giving rise to polarized and depolarized light scattering from gaseous H₂S have been understood, notwithstanding the simple model of the interaction potential that had to be used. The main features of the isotropic induced spectrum can be taken into account on the basis of the usual point-scatterer approximation and no diffuse polarizability model seems to be necessary, at least at low density. The high-frequency tail of the spectrum reflects the molecular nature of the scatterers and their rotational dynamics probed via multipolar polarizabilities, whereas the low-frequency peak is related to translational motions as for anisotropic spectra of globular molecules. Previous measurements at the liquid density[36] showed a central peak and a broad spectrum and can be interpreted on the basis of the present scheme, although a complete analysis requires further theoretical investigations.

Finally, we want to point out that a similar situation is expected for gaseous H₂O at high temperature owing to the similarity in structure and polarizability between H₂O and H₂S molecules.

ACKNOWLEDGMENT

APPENDIX A: MODEL ESTIMATE OF THE DIPOLE-QUADRUPOLE POLARIZABILITY

The H₂S molecule belongs to the C_{2v} point group, and the tensors β, A and γ have three, four, and six indepen-

dent components, respectively.[38,56] In Table III all the molecular properties of H₂S, of interest in this work, are reported in esu units together with conversion factors to SI. Nonzero spherical components have been derived from Cartesian components.[42,57,58]

To get an estimate of the A components which are unknown at all, we have used the model proposed by Applequist et al.:[21,22] each atom of a molecule is regarded as an isotropic polarizable point which interacts with all the others via the dipolar field. The induced dipole on the ith atom is given by

$$\mu_i = \alpha_i \left[\mathbf{E}_i + \sum_{j \neq i} \mathbf{T}_{ij} \mu_j \right] , \qquad (A1)$$

where the sum runs over the N atoms of the molecule, $\mathbf{T} = (1/r^3)[3(\mathbf{rr})/r^2 - \mathbf{1}]$ is the dipole tensor, and $\mathbf{E}$ is the external field on the ith atom with polarizability α_i. Equation (A1) can formally be rewritten as

$$\sum \mathbf{D}_{ij} \mu_j = \mathbf{E}_i , \qquad (A2)$$

where

$$\mathbf{D}_{ij} = \alpha_i^{-1} \delta_{ij} - \mathbf{T}_{ij} (1 - \delta_{ij}) . \qquad (A3)$$

By solving Eq. (A2) for μ_i, one has

$$\mu_i = \sum_j \mathbf{B}_{ij} \mathbf{E}_j . \qquad (A4)$$

The knowledge of the $3N \times 3N$ matrix $\mathbf{B}$ leads to the evaluation of the molecular polarizability α by assuming the external field to be constant over molecular size:

$$\alpha = \sum_{ij} \mathbf{B}_{ij} . \qquad (A5)$$

For a homonuclear diatomic the polarizability components can be written as

$$\alpha_{||} = \frac{2\alpha_a r_0^3}{r_0^3 - 2\alpha_a} , \qquad (A6)$$

$$\alpha_\perp = \frac{2\alpha_a r_0^3}{r_0^3 + \alpha_a} , \qquad (A7)$$

where α_a is the atomic site polarizability. Consequently, a pair of interacting atoms have isotropic $a(r)$ and anisotropic $b(r)$ fluctuating polarizabilities

$$a(r) = \frac{1}{3}(\alpha_{||} + 2\alpha_\perp) - 2\alpha_a = \frac{4\alpha_a^3}{r^6 - \alpha_a r^3 - 2\alpha_a^2} , \qquad (A8)$$

$$b(r) = \alpha_{||} - \alpha_\perp = \frac{6\alpha_a^2 r^3}{r^6 - \alpha_a r^3 - 2\alpha_a^2} . \qquad (A9)$$

Higher-order-induced multipoles can be derived from the model. The quadrupole moment of a system of charges q_k is defined as[38]

$$\Theta_{\alpha\beta}^{(0)} = \frac{1}{2} \sum_k q_k [3 r_\alpha^{(k)} r_\beta^{(k)} - (r^{(k)})^2 \delta_{\alpha\beta}] . \qquad (A10)$$

If a dipole μ is induced in the ith site, the induced quadrupole is[22]

$$\Theta_{\alpha\beta} = \tfrac{1}{2} \sum_i (3 r_\beta^{(i)} \mu_\alpha^{(i)} + 3 r_\alpha^{(i)} \mu_\beta^{(i)} - 2 r_\alpha^{(i)} \mu_\alpha^{(i)} \delta_{\alpha\beta}) . \quad \text{(A11)}$$

From Eq. (A4) one has

$$\Theta_{\alpha\beta} = A_{\alpha\beta,\gamma} E_\gamma$$

$$= \sum_i \left\{ \frac{3}{2} \left[r_\beta^{(i)} \left[\sum_j \mathbf{B}_{ij} \right]_{\alpha\gamma} + r_\alpha^{(i)} \left[\sum_j \mathbf{B}_{ij} \right]_{\beta\gamma} \right] \right.$$

$$\left. - r_\alpha^{(i)} \left[\sum_j \mathbf{B}_{ij} \right]_{\alpha\gamma} \delta_{\alpha\beta} \right\} E_\gamma . \quad \text{(A12)}$$

The values of $A_{\alpha\beta,\gamma}$ can be calculated from the sites positions and atomic site's polarizabilities contained in the tensor **B**. As a preliminary test, we have applied the model to the H_2O molecule whose **A** components are known from *ab initio* calculations.[59] Applequist *et al.*[21] have determined atom polarizabilities by fitting the molecular isotropic polarizability of a large number of molecules. Using the site polarizabilities α_H and α_O of the O—H bond[21] the order of magnitude of the **A** components is reproduced satisfactorily (see Table IV). The model does not reproduce the molecular polarizability anisotropy which is better accounted for by some improved versions.[60] The site polarizabilities α_H and α_S of the H—S bond are not known. Three reasonable values of α_H and α_S fitting the isotropic polarizability are used in order to estimate the **A** components of H_2S molecule (see Table IV). As in the case of H_2O, the anisotropic polarizability is poorly reproduced.

APPENDIX B: ISOTROPIC SPECTRUM EVALUATION

To calculate the Raman rotational transitions of an asymmetric rotor in the ground state, the rotational quantum state $| r \rangle$ has been developed on the basis of the symmetric rotor eigenfunctions

$$| r \rangle = | J\tau M \rangle = \sum_k C_K(J\tau) | JKM \rangle , \quad \text{(B1)}$$

where[61]

$$| JKM \rangle = \left[\frac{2J+1}{8\pi^2} \right]^{1/2} \mathscr{D}_{M,K}^{J*} . \quad \text{(B2)}$$

The eigenvalues problem

$$H \, | r \rangle = H \, | J\tau M \rangle = E_r \, | J\tau M \rangle \quad \text{(B3)}$$

has been resolved by using the Watson's A-reduction Hamiltonian[62,63] in I^r coordinate representation[64] with centrifugal corrections up to tenth order.[63] The intensities of the rotational Raman transitions, due to the zz component of the polarizability tensor α are proportional to the square of the matrix elements

$$\langle J\tau M \, | \alpha_{12,m} \, | J'\tau'M' \rangle$$

$$= \frac{[(2J+1)(2J'+1)]^{1/2}}{8\pi^2}$$

$$\times \sum_{KK'} C_K^* C_{K'}' \langle \mathscr{D}_{M,K}^J \, | \alpha_{12,m} \, | \mathscr{D}_{M',K'}^{J'*} \rangle , \quad \text{(B4)}$$

where $\alpha_{12,m}$ is given by Eq. (21). Rotational Rayleigh spectra of the H_2S molecule have been studied in Ref. 52 and the other allowed bands in Ref. 65. In the present case, the pair polarizability of Eq. (7) is involved in the scattering mechanism. If dynamic orientational variables are assumed to be uncorrelated and rotational states to be independent of the intermolecular distance $\mathbf{R}_{ij}$ the matrix element of $^{\alpha A}\Pi_{10,0}^{(ij+ji)}$ results:

$$W_0 = \langle Q_{ij} \, | ^{\alpha A}\Pi_{10,0}^{(ij+ji)} \, | Q_{ij}' \rangle$$

$$= -\frac{2\sqrt{10/3}}{4\pi\epsilon_0} \alpha \sum_m V_{t,t'}^{(ij)m} \sum_p A_{123,p} (W_{r,r'}^{(i)m,p} + W_{r,r'}^{(j)m,p}) ,$$

$$V_{t,t'}^{(ij)m} = \langle t^{(ij)} \, | (-1)^m \mathscr{D}_{m,0}^{3*}(\Omega_{ij}) R_{ij}^{-4} \, | t'^{(ij)} \rangle , \quad \text{(B5)}$$

$$W_{r,r'}^{(i)m,p} = \langle r^{(i)} \, | \mathscr{D}_{-m,p}^{3*}(\Omega_i) \, | r'^{(i)} \rangle ,$$

where $| Q_{ij} \rangle = | t_{ij} \rangle | r_i \rangle | r_j \rangle$ is the quantum state of the pair, $| r_i \rangle$ being the rotational state of the ith molecule. From Eq. (B2) we obtain

$$W_{r,r'}^{m,p} = \frac{[(2J+1)(2J'+1)]^{1/2}}{8\pi^2}$$

$$\times \sum_{KK'} C_K^* C_{K'}' \langle \mathscr{D}_{M,K}^J \, | \mathscr{D}_{-m,p}^{3*}(\Omega) \, | \mathscr{D}_{M',K'}^{J'*} \rangle . \quad \text{(B6)}$$

By exploiting the properties of the Wigner functions,[66]

$$\langle \mathscr{D}_{M,K}^J \, | \mathscr{D}_{-m,p}^{3*} \, | \mathscr{D}_{M',K'}^{J'*} \rangle = \int \mathscr{D}_{M,K}^J \mathscr{D}_{-m,p}^{3*} \mathscr{D}_{M',K'}^{J'*} d\Omega = 8\pi^2 (-1)^{K-M} \begin{bmatrix} J' & 3 & J \\ K' & p & -K \end{bmatrix} \begin{bmatrix} J' & 3 & J \\ M' & -m & -M \end{bmatrix} , \quad \text{(B7)}$$

one has

$$W_{r,r'}^{m,p} = [(2J+1)(2J'+1)]^{1/2} (-1)^{-M} \begin{bmatrix} J' & 3 & J \\ M' & -m & M \end{bmatrix} \sum_{KK'} C_K^* C_{K'}' (-1)^K \begin{bmatrix} J' & 3 & J \\ K' & p & -K \end{bmatrix} . \quad \text{(B8)}$$

If translations are evaluated classically, the following expression for the polarizability correlation function results:

$$^{\alpha A}C_{VV}^{iso}(t) = \frac{40}{63} \frac{\rho^2 \alpha^2}{(4\pi\epsilon_0)^2} \left\langle \frac{\mathscr{D}_{0,0}^3 [\delta\Omega_{1,2}(t)]}{R_{1,2}^4(t) R_{1,2}^4(0)} \right\rangle_{\text{av}} \sum_{\tau\tau'} \left\langle \left| \sum_p A_{123,p} W_{r,r'}^p \right|^2 \cos\left[\frac{(E_{r'} - E_r)t}{\hbar} \right] \right\rangle_{\text{av}} , \quad \text{(B9)}$$

where $\langle \ \rangle_{\text{av}}$ stands for thermodynamical averages and

$$\left| \sum_p A_{123,p} W_{rr'}^p \right|^2 = \left| \sum_p A_{123,p} \sum_{KK'} C_K^* C_{K'} (-1)^K \begin{bmatrix} J' & 3 & J \\ K' & p & -K \end{bmatrix} \right|^2 . \tag{B10}$$

By Fourier transforming Eq. (B9) one has

$$_{\alpha A} I^{\mathrm{iso}}(v) \propto \frac{40}{63} \frac{\rho^2 \alpha^2}{(4\pi\epsilon_0)^2} \langle R_{1,2}^{-8} \rangle_{\mathrm{av}} \sum_{rr'} \left[\frac{g_r \exp\left[-\dfrac{E_r}{k_B T} \right]}{Z} \left| \sum_p A_{123,p} W_{rr'}^p \right|^2 \delta\left[v - \frac{(E_{r'} - E_r)}{hc} \right] \right] \otimes G_3(v) , \tag{B11}$$

$$G_3(v) \propto F\left[\left\langle \frac{\mathcal{D}_{0,0}^3[\delta\Omega(t)]}{R_{1,2}^4(t) R_{1,2}^4(0)} \right\rangle_{\mathrm{av}} \right] ,$$

$$Z = \sum_r g_r \exp\left[-\frac{E_r}{k_B T} \right] ,$$

where F denotes the Fourier transform, v is the frequency in cm^{-1}, g_r is the spin degeneracy of the state $| r \rangle$, and $\otimes$ stands for the convolution operator. It must be noted that no transitions are obtained at zero frequency in the case of asymmetric rotors (see Fig. 6) in contrast to spherical tops,[17] whose energy levels E_{JKM} are independent of K (and M).

[1] L. Silberstein, Philos. Mag. **33**, 92 (1927).

[2] G. C. Tabisz, *Specialistic Periodical Reports* (British Chemical Society, 1979), Vol. 29.

[3] L. Frommhold, Adv. Chem. Phys. **46**, 1 (1981).

[4] K. L. Clarke, P. A. Madden, and A. D. Buckingham, Mol. Phys. **36**, 301 (1978).

[5] K. L. C. Hunt, J. Chem. Phys. **80**, 393 (1984).

[6] M. H. Proffitt, J. W. Keto, and L. Frommhold, Can. J. Phys. **59**, 1459 (1981).

[7] B. J. Alder, H. L. Strauss, and J. J. Weiss, J. Chem. Phys. **59**, 1002 (1973).

[8] P. A. Madden, Mol. Phys. **36**, 365 (1978).

[9] B. Guillot, S. Bratos, and G. Birnbaum, Phys. Rev. A **22**, 695 (1984).

[10] A. De Santis, M. Sampoli, and R. Vallauri, Mol. Phys. **53**, 695 (1984).

[11] F. Barocchi and J. P. McTague, Phys. Lett. A **53**, 488 (1975).

[12] H. A. Posh and T. A. Litovitz, Mol. Phys. **32**, 1559 (1972).

[13] A. D. Buckingham and G. C. Tabisz, Opt. Lett. **1**, 220 (1977); Mol. Phys. **36**, 583 (1978).

[14] D. P. Shelton and G. C. Tabisz, Mol. Phys. **40**, 1137 (1980).

[15] H. A. Posh, Mol. Phys. **37**, 1059 (1979); **40**, 1137 (1980).

[16] H. A. Posh, Mol. Phys. **46**, 1213 (1982).

[17] A. R. Penner, N. Meinander, and G. C. Tabisz, Mol. Phys. **54**, 479 (1985).

[18] R. A. Stuckart, C. J. Montrose, and T. A. Litovitz, Faraday Discuss. Chem. Soc. **11**, 94 (1977).

[19] M. Neumann, Mol. Phys. **53**, 187 (1984).

[20] M. Neumann and H. A. Posh, *Phenomena Induced by Intermolecular Interactions*, edited by G. Birnbaum (Plenum, New York, 1984).

[21] J. Applequist, J. R. Carl, and K.-K. Fung, J. Am. Chem. Soc. **94**, 2952 (1972).

[22] J. Applequist, Acc. Chem. Res. **10**, 79 (1977).

[23] T. Keyes and B. M. Ladanyi, Mol. Phys. **33**, 1271 (1977).

[24] B. M. Ladanyi and T. Keyes, J. Chem. Phys. **68**, 3217 (1978).

[25] B. M. Ladanyi, T. Keyes, D. J. Tildesley, and W. B. Street, Mol. Phys. **39**, 645 (1980).

[26] B. M. Ladanyi and T. Keyes, J. Chem. Phys. **76**, 2047 (1982).

[27] B. M. Ladanyi, J. Chem. Phys. **78**, 2189 (1983); B. M. Ladanyi and N. E. Levinger, *ibid.* **81**, 2620 (1984).

[28] A. De Santis and M. Sampoli, Mol. Phys. **53**, 717 (1984).

[29] T. I. Cox and P. A. Madden, Mol. Phys. **39**, 1487 (1980).

[30] P. A. Madden and D. J. Tildesley, Mol. Phys. **49**, 193 (1983).

[31] R. D. Amos, A. D. Buckingham, and J. H. Williams, Mol. Phys. **39**, 1519 (1980).

[32] F. G. Baglin, U. Zimmerman, and H. Versmold, Mol. Phys. **52**, 877 (1984).

[33] M. Monan, J. L. Bribes, and R. Gaufrès, J. Chim. Phys. Phys. Chim. Biol. **78**, 781 (1981); J. Mol. Struct. **79**, 83 (1982); J. Raman Spectrosc. **12**, 190 (1982).

[34] A. De Lorenzi, A. De Santis, R. Frattini, and M. Sampoli, J. Mol. Spectrosc. **115**, 156 (1986).

[35] G. Briganti, V. Mazzacurati, G. Ruocco, G. Signorelli, and M. Nardone, Mol. Phys. **49**, 1179 (1983).

[36] A. De Santis and M. Sampoli, Chem. Phys. Lett. **102**, 425 (1983).

[37] A. D. Buckingham, Trans. Faraday Soc. **52**, 1035 (1956).

[38] A. D. Buckingham, Adv. Chem. Phys. **12**, 107 (1967).

[39] A. D. Buckingham and M. J. Stephen, Trans. Faraday Soc. **53**, 884 (1957).

[40] S. Kielich, Acta Phys. Pol. **19**, 149 (1960); **19**, 711 (1960); Mol. Phys. **9**, 549 (1965); Acta Phys. Pol. **27**, 305 (1965); **28**, 459 (1965); J. Chem. Phys. **46**, 4090 (1967); Opt. Commun. **34**, 367 (1980).

[41] R. Samson, R. A. Pasmanter, and A. Ben Reuven, Phys. Rev. A **14**, 1224 (1976); R. A. Pasmanter, R. Samson, and A. Ben Reuven, *ibid.* **14**, 1238 (1976).

[42] A. J. Stone, Mol. Phys. **29**, 1461 (1975).

[43] A more general form of Eq. (7) has been reported in Ref. 29 in the case of Raman bands.

[44] A. Ben Reuven and N. D. Gershon, J. Chem. Phys. **51**, 893 (1969).

[45] H. W. Schrötter and H. W. Klöckner, *Raman Spectroscopy of Gases and Liquids*, edited by A. Weber (Springer-Verlag, Berlin, 1979).

[46] *Enciclopedie des gaz, l'air liquide* (Elsevier, Amsterdam, 1976); H. J. Neuburg, J. F. Atherley, and L. G. Walker, *Girdler Sul-*

phide Process Physical Properties (Atomic Energy of Canada Ltd., Ontario, 1977).

[47]A. De Santis and M. Sampoli, Chem. Phys. Lett. **96**, 114 (1983).

[48]At the resolution of 7 cm^{-1}, the instrumental function has a trapezoidal profile. An accurate analysis of the rotational line shape has been performed in Ref. 34 and here we have not tried to reproduce faithfully the experimental spectrum. The adopted Gaussian profile of the instrumental function allows a satisfactory qualitative reproduction of the experimental spectra.

[49]L. Frommhold, K. H. Hong, and M. H. Proffitt, Mol. Phys. **35**, 665 (1978).

[50]The values of ϵ/k_B and σ used in this work have been calculated in Ref. 35 by scaling the argon values to the corresponding state principle. They are in agreement with the values deduced from viscosity data: J. O. Hirschfelder, C. F. Curtiss, and R. B. Bird, *Molecular Theory of Gases and Liquids* (Wiley, New York, 1964).

[51]A. D. Buckingham and J. A. Pople, Trans. Faraday Soc. **51**, 1173 (1955).

[52]A. De Lorenzi, A. De Santis, R. Frattini, and M. Sampoli, J. Mol. Phys. (to be published).

[53]*Handbook of Chemistry and Physics*, 60th ed. (CRC, Boca Raton, Florida, 1979).

[54]N. Meinander, A. R. Penner, U. Bafile, F. Barocchi, M. Zoppi, D. P. Shelton, and G. C. Tabisz, Mol. Phys. **54**, 493 (1985).

[55]H. Versmold, Mol. Phys. **43**, 383 (1981).

[56]A. D. Buckingham and B. J. Orr, Q. Rev. Chem. Soc. **21**, 195 (1967).

[57]M. E. Rose, *Elementary Theory of Angular Momentum* (Wiley, New York, 1957).

[58]P. D. Maker, Phys. Rev. A **1**, 923 (1976).

[59]I. G. John, G. B. Backsay, and N. S. Hush, Chem. Phys. **51**, 49 (1980).

[60]R. R. Birge, J. Chem. Phys. **72**, 5312 (1980); B. T. Thole, Chem. Phys. **59**, 341 (1981).

[61]L. Landau and E. Lifchitz, *Mécanique Quantique* (Mir, Moscow, 1974).

[62]L. Larrabee Strow, J. Mol. Spectrosc. **97**, 9 (1983).

[63]J. M. Flaud, C. Camy-Peyret, and J. W. C. Johns, Can. J. Phys. **61**, 1462 (1983).

[64]G. W. King, R. M. Hainer, and P. C. Cross, J. Chem. Phys. **11**, 27 (1943).

[65]V. Mazzacurati, M. A. Ricci, G. Ruocco, G. Signorelli, M. Nardone, A. De Santis, and M. Sampoli, Mol. Phys. **54**, 1229 (1985).

[66]A. R. Edmonds, *Angular Momentum in Quantum Mechanics* (Princeton University Press, New Jersey, 1957).

[67]R. L. Cook, F. C. De Lucia, and P. Helminger, J. Mol. Struct. **28**, 237 (1975).

[68]C. G. Gray and K. E. Gubbins, *Theory of Molecular Fluids* (Clarendon, Oxford, 1984), Vol. 1.

[69]M. P. Bogaard, A. D. Buckingham, and G. L. D. Ritchie, Chem. Phys. Lett. **90**, 183 (1982).

[70]J. F. Ward and C. K. Miller, Phys. Rev. A **19**, 826 (1979).